Journal of Fluids and Structures 28 (2012) 483–487

Contents lists available at SciVerse ScienceDirect

Journal of Fluids and Structures

journal homepage: www.elsevier.com/locate/jfs

Nonlinear evolution of instabilities behind spheres and disks

P. Szaltys [a], M. Chrust [a], A. Przadka [a], S. Goujon-Durand [b], L.S. Tuckerman [b,*], J.E. Wesfreid [b]

[a] Warsaw University of Technology, Institute of Aeronautics and Applied Mechanics, Ul Nowowiejska 24, 00665 Warsaw, Poland
[b] PMMH (UMR 7636 CNRS - ESPCI - Univ. Paris 6 - Univ. Paris 7), 10 rue Vauquelin, 75005 Paris, France

ARTICLE INFO

Article history:
Received 18 November 2010
Received in revised form
11 April 2011
Accepted 20 April 2011
Available online 30 November 2011

Keywords:
Wake
Sphere
Disk
Bluff body
Hairpin
Vortex

ABSTRACT

We have performed precise and systematic experiments with PIV in order to measure the velocity field in the wake of a solid sphere and of a disk in a water channel, in the range of intermediate Reynolds number in which stationary and oscillatory instabilities appear, including the hairpin shedding regime. From these experimental data, we study the modal decomposition of the streamwise vorticity in an unsteady case and we describe the full nonlinear evolution of the bifurcating branches. We compare these results with recent theoretical and numerical studies on instability in the vortex shedding process at these intermediate Reynolds numbers.

1. Background

The flow behind a sphere and a disk has been investigated experimentally with flow visualization and particle image velocimetry (PIV). We have observed in the two cases how the steady axisymmetric flow with toroidal recirculation zone behind the body bifurcates to a steady flow with a planar symmetry containing two longitudinal counter-rotating vortices. A further instability leads to oscillation of these vortices, and for larger Reynolds numbers, to unsteady flow with regular hairpin shedding (Ghidersa and Dusek, 2000; Johnson and Patel, 1999; Magarvey and Bishop, 1961; Natarajan and Acrivos, 1993; Schouveiler and Provensal, 2002; Tomboulides and Orszag, 2000).

2. Experimental set-up

Our experiments have been carried out in a low-velocity water channel with a 10×10 cm cross-section, a typical velocity of 0.4–4 cm/s and the Reynolds number of 100–450 for the sphere and 50–500 for the disk. The sphere has a diameter of $d=1.6$ cm. The disk has a diameter of $d=1.2$ cm with a thickness of $h=0.2$ cm, i.e. aspect ratio $d/h=6$ or $h/d=0.167$. (We also present some measurements for d/h ranging from 1 to 33.) In both cases, the body was held from upstream by nearly horizontal rigid bent tubes. The wake was visualized using laser induced fluorescein. The dye was injected through a hole in the middle of the disk and with a central horizontal slit in the downstream face of the sphere. The velocity fields were measured using a standard particle image velocimetry set-up.

DOI of original articles: 10.1016/j.jfluidstructs.2011.04.005, 10.1016/j.jfluidstructs.2011.09.001
* Corresponding author.
E-mail addresses: sophie@pmmh.espci.fr (S. Goujon-Durand), laurette@pmmh.espci.fr (L.S. Tuckerman), wesfreid@pmmh.espci.fr (J.E. Wesfreid).

0889-9746/$ - see front matter © 2011 Elsevier Ltd. All rights reserved.
doi:10.1016/j.jfluidstructs.2011.10.004

3. Experimental observations

From Reynolds number greater than 212 for the sphere and 125 for the disk, the flow loses axisymmetry and two steady counter-rotating vortices appear with a plane of symmetry, as shown in Fig. 1(a) in the case of the disk. We note that the transitions for the disk depend on the aspect ratio, as previously shown by Fernandes et al. (2007), and seen in Fig. 3 (Bobinski, 2011).

Starting at Re=268 for the sphere and Re=137 for the disk, regular oscillations are observed. The Strouhal number $St=fd/U$ at onset is 0.18 for the sphere and 0.16 for the disk, and varies little (less than 10%) with the Reynolds number. Subsequently, for Re $\gtrsim$ 272 for the sphere (Gumowski et al., 2008; Przadka et al., 2008) and Re $\gtrsim$ 142 for the disk, in which oscillations are related only to the vacillation of the counter-rotating vortices, the visualizations from the side view show the form of one-sided hairpins, as in Fig. 1(b). For the disk, for Re $>$ 175, the top view shows small irregularities midway between hairpin heads, as in Fig. 1(c). Fig. 2 displays the wake of a sphere, with dye visualization showing the hairpins.

PIV measurements were performed for the same experimental conditions. Our water tunnel allows optical access to the back view, by means of which we measured the streamwise vorticity. We observe pairs of steady counter-rotating vortices whose amplitude increases with the Reynolds number. A typical periodic cycle is depicted in Fig. 4, which shows a color

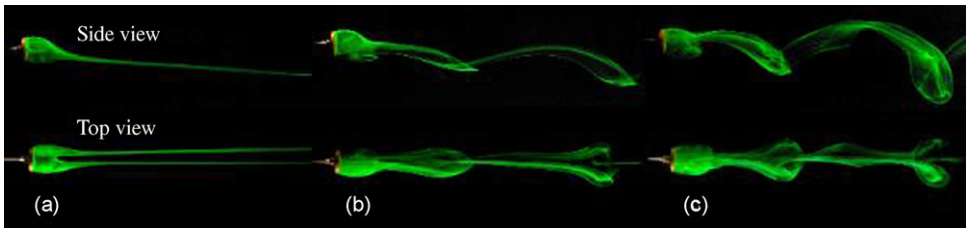

Fig. 1. Flow visualization of the wake behind a disk. (a) Steady flow at Re=125, (b) regular hairpin shedding at Re=165, and (c) regular hairpin shedding and irregularity midway between hairpin heads at Re=210.

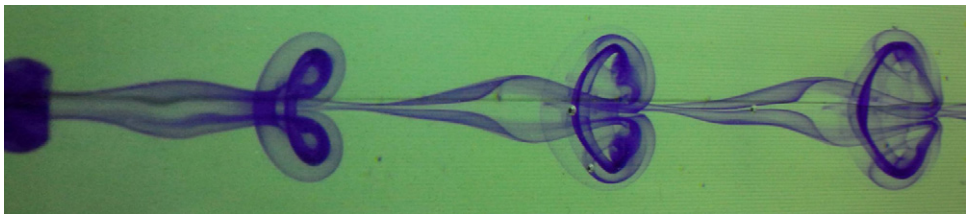

Fig. 2. Wake behind sphere in hairpin-shedding regime.

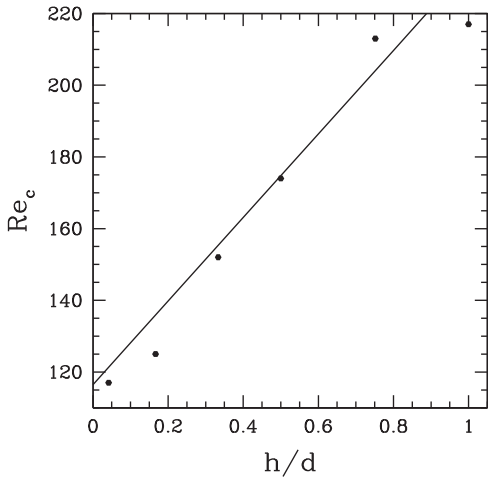

Fig. 3. Aspect-ratio dependence of critical Reynolds number for loss of axisymmetry in the wake behind a disk. The dots indicate our experimental observations, while the line is the fit $Re_c = 116.5(1+h/d)$ proposed by Fernandes et al. (2007) based on their numerical simulations.

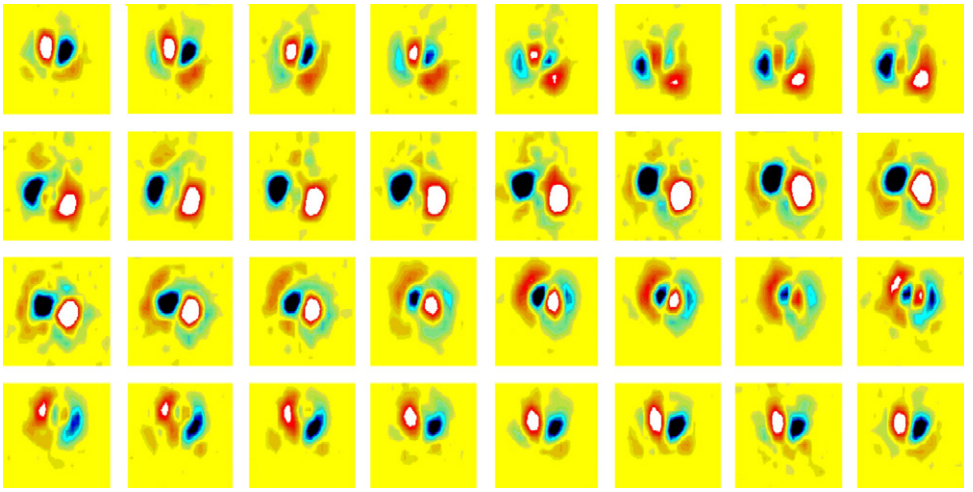

Fig. 4. PIV measurements from a rear view showing the axial vorticity behind the disk during one oscillation period of the flow at Re=210. The measurement plane is 2.5*d* downstream from the disk.

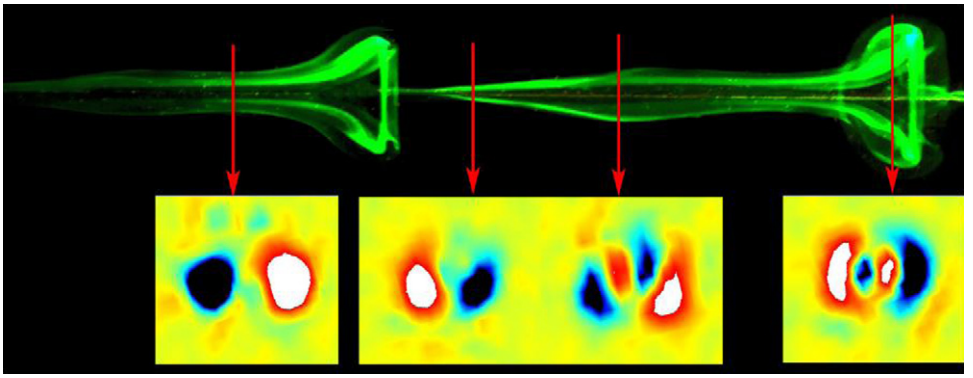

Fig. 5. Correspondence between side view obtained via LIF and transverse view obtained via PIV in the wake of a disk at Re ≈ 210. The PIV measurements are taken at a single spatial location at different times. The arrows identify the spatial locations in the side view which correspond to the temporal phases of the wake in the transverse views.

Fig. 6. Axial vorticity of modes $m=1$ (left), $m=2$ (middle), and $m=3$ (right) from an instantaneous field measured at 2.5*d* downstream from the sphere at Re=300. Dark and light correspond to positive and negative vorticities, respectively, with the intensity for each figure scaled separately.

map of the axial vorticity as a function of time during one oscillation cycle. Fig. 5 shows the correspondence between the side view obtained via LIF and the transverse view obtained via PIV at different instants of the cycle, by identifying spatial locations in the side view at which the transverse view resembles the pictures shown below.

4. Modal decomposition

To study the evolution of the flow field as the Reynolds number is increased, we decomposed the axial vorticity Ω into its azimuthal Fourier components by a sequence of direct and inverse transforms:

$$\Omega^{\mathrm{Cart}}(x_j,y_k)\rightarrow\hat{\Omega}^{\mathrm{Cart}}(j',k')\rightarrow\Omega^{\mathrm{polar}}(r_\ell,\theta_n)\rightarrow\hat{\Omega}^{\mathrm{polar}}(r_\ell,m)\rightarrow\hat{\Omega}_m. \tag{1}$$

More specifically, starting from the PIV measurements $\Omega^{\mathrm{Cart}}(x_j,y_k)$ provided on a Cartesian grid in a transverse plane, we use a 2-D Cartesian Fourier transform to interpolate onto the polar grid, $\Omega^{\mathrm{polar}}(r_\ell,\theta_n)$:

$$\hat{\Omega}^{\mathrm{Cart}}(j',k')\equiv\sum_j\sum_k\Omega^{\mathrm{Cart}}(x_j,y_k)\mathrm{e}^{-\mathrm{i}(j'x_j+k'y_k)}, \tag{2}$$

$$\Omega^{\mathrm{polar}}(r_\ell,\theta_n)\equiv\sum_{j'}\sum_{k'}\hat{\Omega}^{\mathrm{Cart}}(j',k')\mathrm{e}^{\mathrm{i}(j'r_\ell\cos\theta_n+k'r_\ell\sin\theta_n)}. \tag{3}$$

We then perform a 1D polar Fourier transform followed by a discrete radial integral:

$$\hat{\Omega}^{\mathrm{polar}}(r_\ell,m)\equiv\sum_n\Omega^{\mathrm{polar}}(r_\ell,\theta_n)\mathrm{e}^{-\mathrm{i}m\theta_n}, \tag{4}$$

$$\hat{\Omega}_m\equiv\sum_\ell\hat{\Omega}^{\mathrm{polar}}(r_\ell,m)r_\ell\Delta r. \tag{5}$$

Fig. 6 shows an example of this decomposition of an instantaneous snapshot of the axial vorticity. The field associated with mode m is $\hat{\Omega}^{\mathrm{polar}}(r,m)e^{\mathrm{i}m\theta}$.

As Re is increased past 268 for the sphere and 137 for the disk, the flow becomes periodic, as do the coefficients $\hat{\Omega}_m$, with more complicated temporal behavior seen at still higher Re. In these cases we compute the maximum over time of the Fourier components $\max_t\hat{\Omega}_m(t)$. Fig. 7(a) shows the importance of the $m=1$ dipole component. An experimental bifurcation diagram using $\max_t|f_1(t)|^2=\max_t|\hat{\Omega}_{m=1}(t)|^2$ is shown in Fig. 7(b) for the sphere. A bifurcation diagram for the disk containing modes 0 through 4 is presented in Fig. 8.

The results of recent numerical and theoretical investigations (Bouchet et al., 2006; Fabre et al., 2008; Gushchin and Matyushin, 2006; Meliga et al., 2009; Pier, 2008; Shenoy and Kleinstreuer, 2008) display a similar sequence of transitions. Our experimental observations overlap with, and extend, the Reynolds number range of these investigations. We observe a strong increase in the Fourier mode $m=3$ at Re=185 in the wake of the disk. This new bifurcation coincides with the visual observation of what have been termed two-sided hairpins or alternating shedding hairpins.

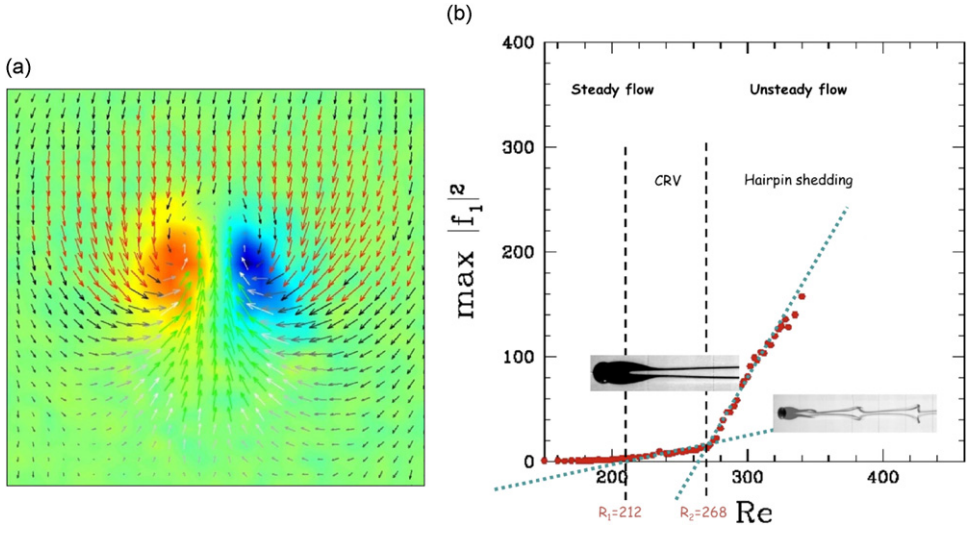

Fig. 7. (a) Pair of counter-rotating axial vortices in the instantaneous flow behind a sphere. Arrows: transverse velocity field measured by PIV. Shading: axial vorticity. (b) Maximum amplitude over time of dipole mode $\max_t|f_1(t)|^2=\max_t|\hat{\Omega}_{m=1}(t)|^2$. The slope increases at Re=212, signaling the breaking of axisymmetry, and again at Re=268, signaling the onset of time dependence.

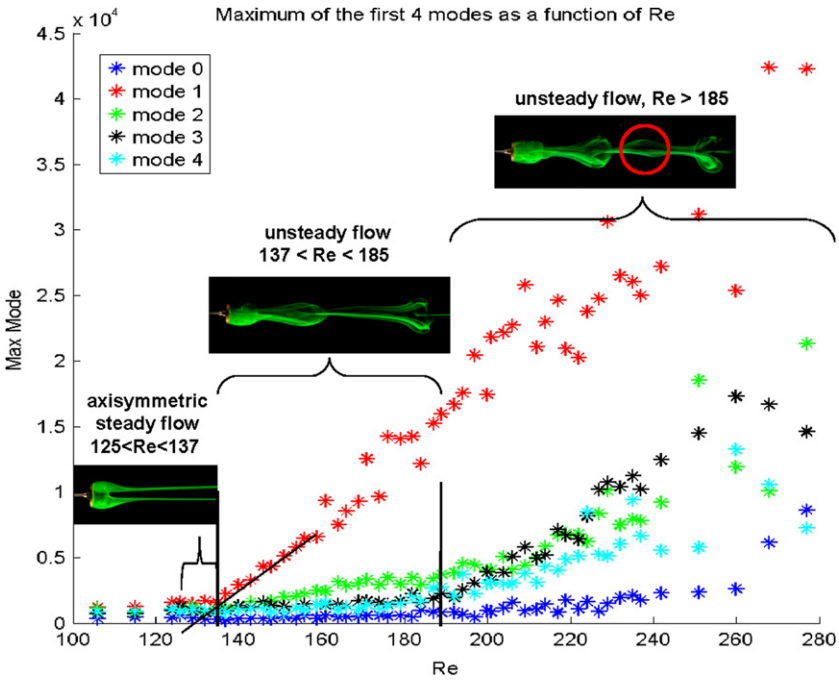

Fig. 8. Modal decomposition of axial vorticity in wake behind a disk as a function of Re. The maximum over time of azimuthal modes 0, 1, 2, 3, 4 are shown, along with visualizations in the steady and unsteady regimes. Thresholds are identified via these graphs or by flow visualization. Increases in slope in the $m=1$ component can be seen at the Reynolds numbers near 125 and 137, corresponding to the breaking of axisymmetry and the onset of time dependence, respectively. An increase in slope in the $m=3$ component can be seen at $\mathrm{Re}\approx 185$.

References

Bobinski, T., 2011. Private communication.

Bouchet, G., Mebarek, M., Dušek, J., 2006. Hydrodynamic forces acting on a rigid fixed sphere in early transitional regimes. European Journal of Mechanics B/Fluids 25, 321–336.

Fabre, D., Auguste, F., Magnaudet, J., 2008. Bifurcation and symmetry breaking in wake of axisymmetric bodies. Physics of Fluids 20, 051702.

Fernandes, P.C., Risso, R., Ern, P., Magnaudet, J., 2007. Oscillatory motion and wake instability of freely rising axisymmetric bodies. Journal of Fluid Mechanics 573, 479–502.

Ghidersa, B., Dusek, J., 2000. Breaking of axisymmetry and onset of unsteadiness in the wake of a sphere. Journal of Fluid Mechanics 423, 33–69.

Gumowski, K., Miedzik, J., Goujon-Durand, S., Jenffer, P., Wesfreid, J., 2008. Transition to a time-dependent state of fluid flow in the wake of a sphere. Physical Review E 77, 055308.

Gushchin, V.A., Matyushin, R.V., 2006. Vortex formation mechanisms in the wake behind a sphere for $200 < Re < 380$. Fluid Dynamics 41, 795–809.

Johnson, T.A., Patel, V.C., 1999. Flow past a sphere up to a Reynolds number of 300. Journal of Fluid Mechanics 378, 19–70.

Magarvey, R.H., Bishop, R.L., 1961. Transition ranges for three-dimensional wakes. Canadian Journal of Physics 39, 1418–1422.

Meliga, P., Chomaz, J.M., Sipp, D., 2009. Global mode interaction and pattern selection in the wake of disks: a weakly nonlinear expansion. Journal of Fluid Mechanics 633, 159–189.

Natarajan, R., Acrivos, A., 1993. The instability of the steady flow past spheres and disks. Journal of Fluid Mechanics 254, 323–344.

Pier, B., 2008. Local and global instabilities in the wake of a sphere. Journal of Fluid Mechanics 603, 39–61.

Przadka, A., Miedzik, J., Gumowski, K., Goujon-Durand, S., Wesfreid, J., 2008. The wake behind the sphere, analysis of vortices during transition from steadiness to unsteadiness. Archives of Mechanics 60, 467.

Schouveiler, L., Provensal, M., 2002. Self-sustained oscillations in the wake of a sphere. Physics of Fluids 14, 3846–3854.

Shenoy, R., Kleinstreuer, C., 2008. Flow over a thin circular disk at low to moderate Reynolds numbers. Journal of Fluid Mechanics 605, 253–262.

Tomboulides, A.G., Orszag, S.A., 2000. Numerical investigation of transitional and weak turbulent flow past a sphere. Journal of Fluid Mechanics 416, 45–73.